Title

Mechanistic Insights into Temperature-Dependent Trithiocarbonate Chain-End Degradation during the RAFT Polymerization of N-Arylmethacrylamides

Journal

Macromolecules, 49(2)

ISSN

0024-9297

Authors

Abel, Brooks A
McCormick, Charles L

Publication Date

2016-01-26

DOI

10.1021/acs.macromol.5b02463

Peer reviewed

Macromolecules

Article

pubs.acs.org/Macromolecules

Mechanistic Insights into Temperature-Dependent Trithiocarbonate Chain-End Degradation during the RAFT Polymerization of *N*-Arylmethacrylamides

Brooks A. Abel[†] and Charles L. McCormick*[,†,‡]

[†]Department of Polymer Science and Engineering and [‡]Department of Chemistry and Biochemistry, The University of Southern Mississippi, Hattiesburg, Mississippi 39406-5050, United States

Supporting Information

ABSTRACT: Mechanistic insights into trithiocarbonate degradation during the RAFT polymerization of *N*-arylmethacrylamides are reported. Previous work by our group showed significant RAFT agent degradation during the polymerization of *N*-arylmethacryloyl sulfonamides at 70 °C. Herein we report the influence of methacrylamide structure on trithiocarbonate degradation during the RAFT polymerizations of *N*-phenylmethacrylamide (PhMA) and *N*-benzylmethacrylamide (BnMA) in DMF at 70 and 30 °C. UV−vis spectroscopy revealed trithiocarbonate degradation occurs exclusively after covalent addition of monomer to the RAFT agent, with 60% trithiocarbonate degradation occurring after 12 h during the polymerization of PhMA at 70 °C compared to only 3% degradation measured during the polymerization of BnMA under identical conditions. Small molecule analogues of trithiocarbonate-functional poly(PhMA) and poly(BnMA) were synthesized by single monomer unit insertion and the kinetics and byproducts of degradation investigated by *in situ* ^{1}H NMR analysis at 70 °C. Trithiocarbonate degradation was ultimately shown to occur by *N*-phenyl-promoted, N-5 nucleophilic attack on the terminal thiocarbonyl by the ultimate methacrylamide unit.

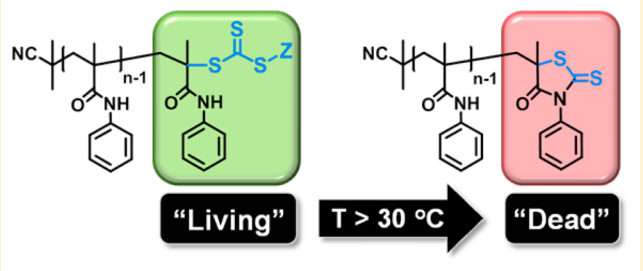

INTRODUCTION

The acknowledged utility of reversible-deactivation radical polymerization (RDRP) is the facile synthesis of polymers with precise compositions, predetermined molecular weights, and well-defined architectures while incorporating monomers possessing a wide variety of functional groups.[1−4] The success of any RDRP technique depends greatly upon maintaining "living" chain end fidelity. In particular, the reversible addition−fragmentation chain transfer (RAFT) process must retain thiocarbonylthio end groups in order to maintain the active/dormant equilibrium necessary for polymerization control. While thiocarbonylthio reactivity has often been exploited as a facile means of postpolymerization end-group modification of RAFT polymers,[5−11] a number of deleterious side reactions involving the thiocarbonylthio moiety can occur including hydrolysis,[12] aminolysis,[12,13] thermolysis,[14] oxidation,[15,16] and irreversible coupling of intermediate radicals.[17−19] It is therefore important to fully understand the nature of any degradative reactions involving thiocarbonylthio end groups in order to extend the current capabilities of RAFT polymerization.

Recently, we reported the RAFT polymerization of a library of pH-responsive methacryloyl sulfonamide (MSA) monomers derived from sulfa drugs.[20] Loss of chain-end functionality was observed during the polymerization of MSAs at the commonly used temperature of 70 °C as evidenced, in part, by broad molecular weight distributions (M_w/M_n > 1.3) and failure to successfully chain extend a poly(MSA) macro-chain-transfer agent (macro-CTA). However, narrow molecular weight distributions and controlled molecular weights were ultimately achieved by conducting the polymerizations at 30 °C. The poor polymerization control of MSAs at 70 °C surprisingly contrasts numerous literature reports of successful RAFT polymerizations of (meth)acrylamides in organic and aqueous media at temperatures greater than 60 °C,[13,21−25] thus prompting our current investigation.

Since our initial report,[20] we have conducted the RAFT polymerization of *N*-phenylmethacrylamide (PhMA), an MSA analogue lacking the sulfonamide functional group (*vide infra*). Notably, the trithiocarbonate-mediated polymerization of PhMA at 70 °C also results in relatively broad molecular weight distributions (M_w/M_n = 1.30), indicating that the sulfonamide functional group is not the primary cause for chain-end degradation during polymerization of MSAs. Previous reports regarding the atom transfer radical polymerization (ATRP) of (meth)acrylamides attributed loss of "living" chain ends to nucleophilic displacement of the terminal bromine by the penultimate amide unit.[26−28] Similarly, oxazolone formation during peptide synthesis occurs by an amide "backbiting" reaction.[29] There is also literature precedent

Received: November 12, 2015
Revised: December 16, 2015
Published: January 4, 2016

DOI: 10.1021/acs.macromol.5b02463
Macromolecules 2016, 49, 465−474

for the effects of *N*-aryl substitution on the cyclization of (thio)carbamoyl derivatives formed during sequencing of peptides by Edman's degradation[30] as well as the cyclization of γ-bromobutyranilides.[31] From these observations, we have hypothesized that a similar reaction involving nucleophilic attack on the ω-thiocarbonyl by the terminal methacrylamide unit may be responsible for thiocarbonylthio degradation during the RAFT polymerization of *N*-arylmethacrylamides.

In this contribution we report the influences of methacrylamide structure and reaction temperature on trithiocarbonate degradation during the RAFT polymerization of N-substituted methacrylamides. A detailed study of the trithiocarbonate-mediated polymerizations of PhMA and *N*-benzylmethacrylamide (BnMA) using SEC-MALLS and UV−vis spectroscopy has now provided a clear understanding of the influence of methacrylamide structure on CTA degradation. Furthermore, *in situ* ^{1}H NMR analysis of RAFT polymer small molecule analogues, prepared by single monomer unit insertion, affords additional mechanistic insight into the specific degradation pathway.

EXPERIMENTAL SECTION

Materials. Methacryloyl chloride (Aldrich, 97%) was vacuum distilled and stored under argon at −10 °C prior to use. Aniline (Aldrich, 99%) and benzylamine (Aldrich, 98%) were vacuum distilled immediately prior to use. 4,4-Azobis(4-cyanovaleric acid) (V501) (Aldrich, 98%) and azobis(isobutyronitrile) (AIBN) (Aldrich, 98%) were recrystallized from methanol and stored at −10 °C. *N*,*N*′-Dimethylformamide (Acros, extra dry w/sieves) was stirred under vacuum at room temperature for 60 min prior to use in order to remove possible traces of dimethylamine. 2,2′-Azobis(4-methoxy-2,4-dimethylvaleronitrile) (V-70) (Wako, 96%), 1-dodecanethiol (Aldrich, 98%), ethanethiol (Aldrich, 97%), carbon disulfide (Aldrich, 99.9%), 2-bromoisobutyryl bromide (TCI, 98%), triethylamine (Aldrich, 99.5%), NaH (Aldrich, 95%), and *N*,*N*′-dimethylformamide-d_7 (Cambridge Isotope, 99.5%) were used as received.

Characterization. NMR spectra for structural analysis and monomer conversions were obtained using a Varian INOVA 300 MHz NMR spectrometer. Polymer molecular weights and molecular weight distributions (M_w/M_n) were determined by size exclusion chromatography (SEC) using DMF 20 mM LiBr as the eluent at a flow rate of 1.0 mL/min in combination with two Agilent PolarGel-M columns heated to 50 °C and connected in series with a Wyatt Optilab DSP interferometric refractometer and Wyatt DAWN EOS multiangle laser light scattering (MALLS) detector (λ = 633 nm). Absolute molecular weights and M_w/M_n were calculated using a Wyatt ASTRA SEC/LS software package. The d*n*/d*c* values for each polymer derivative in the above eluent at 35 °C were determined offline using a Wyatt Optilab DSP interferometric refractometer and Wyatt ASTRA d*n*/d*c* software.

*N-Phenylmethacrylamide (**1**).* Methacryloyl chloride (11.83 mL, 121 mmol) was added dropwise over 15 min to a stirred solution of aniline (12.00 g, 121 mmol) and triethylamine (12.86 g, 127 mmol) in CH_2Cl_2 (250 mL) that was previously cooled using an ice bath. Upon complete addition of methacryloyl chloride, the reaction was stirred at 0 °C for 30 min followed by stirring at room temperature for an additional 60 min. The reaction mixture was then transferred to a separatory funnel and washed with 0.1 N HCl (1 × 200 mL), saturated $NaHCO_3$ (1 × 200 mL), and saturated NaCl (brine) (1 × 200 mL) before drying over $MgSO_4$. The solvent was removed via rotary evaporation, and the isolated solids were recrystallized from hot hexanes:THF (95:5) to yield **1** (17.52 g, 90%) as colorless needle-like crystals; mp 80−81 °C. ^{1}H NMR (300 MHz, $CDCl_3$): δ 7.60 (s, 1H), 7.57 (d, 2H), 7.32 (t, 2H), 7.11 (t, 1H), 5.78 (s, 1H), 5.44 (s, 1H), 2.05 (s, 3H). ^{13}C NMR ($CDCl_3$): δ 166.87, 141.05, 137.95, 129.15, 124.57, 120.24, 120.04, 18.96.

*N-Benzylmethacrylamide (**2**).* A synthetic procedure analogous to that described for **1** was used to prepare *N*-benzylmethacrylamide. The product was recrystallized from hot hexanes:THF (90:10) to yield **2** (17.88 g, 91%) as colorless needle-like crystals; mp 78−79 °C. ^{1}H NMR (300 MHz, $CDCl_3$): δ 7.30 (m, 5H), 6.13 (s, 1H), 5.71 (s, 1H), 5.34 (s, 1H), 4.50 (d, 2H), 1.97 (s, 3H). ^{13}C NMR ($CDCl_3$): δ 168.43, 140.03, 138.41, 128.87, 127.97, 127.67, 119.89, 43.86, 18.89.

*Sodium Dodecyl Trithiocarbonate (**3**).* 1-Dodecanethiol (15.0 g, 74.1 mmol) was added dropwise over 30 min to a stirred suspension of NaH (1.68 g, 70.0 mmol) in anhydrous diethyl ether (350 mL), resulting in slow evolution of hydrogen gas. The reaction mixture was vented and stirred overnight (12 h) at room temperature, after which carbon disulfide (5.64 g, 74.1 mmol) was added dropwise over 10 min, followed by stirring at room temperature for 60 min. The reaction mixture was subsequently diluted with pentane (100 mL), and the solids were isolated by vacuum filtration and further dried *in vacuo* to yield **3** (18.55 g, 83%) as a yellow solid. ^{1}H NMR (300 MHz, DMSO-d_6): δ 2.97 (t, 2H), 1.49 (m, 2H), 1.23 (b, 18H), 0.85 (t, 3H). ^{13}C NMR (DMSO-d_6): δ 31.79, 29.55, 29.51, 29.27, 29.21, 29.14, 22.59, 14.45.

*Bisdodecyl Trithiocarbonate (**4**).* To a suspension of sodium dodecyl trithiocarbonate (18.55 g, 61.7 mmol) in diethyl ether (200 mL) at room temperature was added solid I_2 (8.62 g, 34.0 mmol) over 5 min. The reaction was stirred for 60 min at room temperature followed by removal of the precipitated NaI salts by vacuum filtration. The filtrate was transferred to a separatory funnel and washed with 5% $Na_2S_2O_4$ (1 × 150 mL), H_2O (1 × 150 mL), and brine (1 × 150 mL) before drying over $MgSO_4$. The solvent was removed via rotary evaporation to yield **4** (16.36 g, 96%) as a yellow oil that solidified upon cooling to −10 °C. ^{1}H NMR (300 MHz, $CDCl_3$): δ 3.28 (t, 4H), 1.68 (m, 4H), 1.24 (b, 36H), 0.87 (t, 6H). ^{13}C NMR ($CDCl_3$): δ 221.74, 38.52, 32.13, 29.85, 29.77, 29.64, 29.57, 29.31, 29.16, 27.57, 22.91, 14.36.

*2-Cyano-2-propyldodecyl Trithiocarbonate (**5**).* Bisdodecyl trithiocarbonate (7.88 g, 14.2 mmol) and AIBN (2.33 g, 14.2 mmol) were dissolved in EtOAc (250 mL), and the solution was purged with N_2 for 40 min before heating to 77 °C. After 12 h, a degassed solution of AIBN (2.33 g, 14.2 mmol) in EtOAc (100 mL) was subsequently added, and the reaction mixture was stirred for an additional 12 h at 77 °C. Purification by column chromatography (95:5 hexanes:EtOAc) yielded **5** (7.36 g, 75%) as a yellow oil that solidified upon cooling to 0 °C. ^{1}H NMR (300 MHz, $CDCl_3$): δ 3.32 (t, 2H), 1.86 (s, 6H), 1.68 (m, 2H), 1.25 (b, 18H), 0.87 (t, 3H). ^{13}C NMR ($CDCl_3$): δ 217.96, 120.66, 42.54, 37.13, 32.11, 29.82, 29.74, 29.62, 29.54, 29.27, 29.12, 27.91, 27.25, 22.90, 14.35.

*Sodium Ethyl Trithiocarbonate (**6**).* A suspension of NaH (2.11 g, 83.5 mmol) in anhydrous diethyl ether (150 mL) was cooled to 0 °C using an ice bath; ethanethiol (5.73 g, 92.3 mmol) was then added dropwise over 15 min accompanied by vigorous evolution of hydrogen gas. The reaction mixture was stirred for an additional 15 min at 0 °C followed by dropwise addition of CS_2 (7.03 g, 92.3 mmol) over 5 min, and the reaction mixture was stirred for 60 min at room temperature followed by dilution with pentane (100 mL). The resulting yellow precipitate was isolated by vacuum filtration before drying *in vacuo* yielding **6** (12.07 g, 90%) as a hygroscopic yellow solid. ^{1}H NMR (300 MHz, D_2O): δ 3.15 (q, 2H), 1.27 (t, 3H). ^{13}C NMR (D_2O): δ 35.36, 12.39.

*2-Bromoisobutyranilide (**7**).* 2-Bromoisobutyryl bromide (15.00 mL, 124 mmol) was added dropwise over 15 min to a stirred solution of aniline (12.03 g, 124 mmol) and triethylamine (12.28 g, 124 mmol) in CH_2Cl_2 (500 mL) that was previously cooled using an ice bath. Upon complete addition of 2-bromoisobutyryl bromide, the reaction was stirred at 0 °C for 30 min followed by stirring at room temperature for an additional 60 min. The reaction mixture was then transferred into a separatory funnel and washed with 0.1 N HCl (1 × 400 mL), saturated $NaHCO_3$ (1 × 400 mL), and brine (1 × 400 mL) before drying over $MgSO_4$ and removal of the solvent by rotary evaporation. The isolated solids were recrystallized from hot hexanes to yield **7** (29.13 g, 97%) as colorless needle-like crystals; mp 82−23 °C. ^{1}H NMR (300 MHz, $CDCl_3$): δ 8.45 (s, 1H), 7.55 (d, 2H), 7.35

DOI: 10.1021/acs.macromol.5b02463
Macromolecules 2016, 49, 465−474

(t, 2H), 7.14 (t, 1H), 2.04 (s, 6H). ^{13}C NMR ($CDCl_3$): δ 170.12, 137.53, 129.24, 125.06, 120.11, 63.37, 32.75.

*N-Phenyl-2-(ethylsulfanylthiocarbonylsulfanyl)propanamide (**8**).* A solution of sodium ethyl trithiocarbonate (1.32 g, 8.3 mmol), 2-bromoisobutyrylanilide (2.00 g, 8.3 mmol), and NaI (0.124 g, 0.83 mmol) in absolute EtOH (10 mL) was prepared and stirred at 22 °C for 48 h. The reaction mixture was then precipitated twice into water (100 mL), and the precipitate isolated by vacuum filtration and further purified by recrystallization from absolute EtOH, resulting in large needle-like crystals. The product, isolated by recrystallization, was determined to be 5,5-dimethyl-3-phenyl-2-thioxothiazolidin-4-one (**9**).[32] Conducting the reaction at 60 °C for 12 h allowed for isolation of **9** in higher yields for use in additional studies; mp 108−110 °C. ^{1}H NMR (300 MHz, $CDCl_3$): δ 7.50 (m, 3H), 7.22 (d, 2H), 1.79 (s, 6H). ^{13}C NMR ($CDCl_3$): δ 199.80, 179.64, 135.43, 129.82, 129.70, 128.54, 55.59, 27.55.

*CPDT-PhMA (**10**).* A solution of 2-cyano-2-propyldodecyl trithiocarbonate (3.41 g, 9.9 mmol), PhMA (1.59 g, 9.9 mmol), and V-70 (0.609 g, 2.0 mmol) in DMF (35 mL) was prepared in a round-bottomed flask equipped with magnetic stir bar, and the reaction mixture was degassed via three freeze−pump−thaw cycles and backfilled with argon. The reaction mixture was heated at 30 °C in an oil bath for 48 h, followed by exposure to air and freezing in liquid N_2. The reaction mixture was then diluted with EtOAc (250 mL) and transferred to a separatory funnel and washed with 75% brine (1 × 200 mL), H_2O (1 × 200 mL), and brine (1 × 200 mL) and dried over $MgSO_4$. The crude product was then purified by column chromatography (8:2 hexanes:EtOAc, R_f = 0.30), yielding **10** (0.511 g, 10%) as a yellow solid. ^{1}H NMR (300 MHz, $CDCl_3$): δ 8.44 (s, 1H), 7.45 (d, 2H), 7.32 (t, 2H), 7.12 (t, 1H), 3.26 (t, 2H), 2.55 (q, 2H), 2.02 (s, 3H), 1.64 (m, 2H), 1.47 (s, 3H), 1.46 (s, 3H), 1.23 (b, 18H), 0.87 (t, 3H). ^{13}C NMR ($CDCl_3$): δ 219.02, 169.43, 137.45, 129.02, 124.83, 120.51, 60.48, 45.13, 37.33, 31.91, 30.45, 29.62, 29.54, 29.42, 29.35, 29.10, 29.07, 28.90, 28.69, 27.62, 23.81, 22.70, 14.15.

*CPDT-BnMA (**11**).* A solution of 2-cyano-2-propyldodecyl trithiocarbonate (2.00 g, 5.8 mmol), BnMA (1.01 g, 5.8 mmol), and AIBN (0.190 g, 1.2 mmol) in DMF (20 mL) was prepared in a round-bottomed flask equipped with magnetic stir bar, degassed via three freeze−pump−thaw cycles, and backfilled with argon. The reaction mixture was heated at 60 °C in an oil bath for 24 h, followed by exposure to air and freezing in liquid N_2. The reaction mixture was then diluted with EtOAc (150 mL) and transferred to a separatory funnel and washed with 75% brine (1 × 150 mL), H_2O (1 × 150 mL), and brine (1 × 150 mL) and dried over $MgSO_4$. The crude product was first purified by column chromatography (8:2 hexanes:EtOAc, R_f = 0.25) followed by recrystallization from MeOH:H_2O (98:2) at −10 °C yielding **11** (0.475 g, 16%) as yellow crystals. ^{1}H NMR (300 MHz, $CDCl_3$): δ 7.31 (m, 5H), 6.79 (t, 1H), 4.42 (q, 2H), 3.25 (t, 2H), 2.56 (q, 2H), 1.96 (s, 3H), 1.64 (m, 2H), 1.47 (s, 3H), 1.45 (s, 3H), 1.27 (b, 18H), 0.89 (t, 3H). ^{13}C NMR ($CDCl_3$): δ 219.32, 171.33, 137.62, 128.87, 128.38, 127.84, 125.04, 60.16, 45.04, 37.28, 32.12, 30.66, 29.84, 29.76, 29.64, 29.55, 29.47, 29.29, 29.14, 28.72, 27.87, 24.16, 22.90, 14.35.

RAFT Polymerization of PhMA and BnMA. Briefly, monomer (PhMA or BnMA) (10.0 mmol, 200 equiv), CPDT (5.0×10^{-5} mol, 1 equiv), initiator (V-70 or V501) (1.0×10^{-5} mol, 0.2 equiv), and trimesic acid (50 mg, ^{1}H NMR internal standard) were combined in a 10 mL graduated cylinder, and DMF was added to bring the final solution volume to 5.0 mL ($[M]_0$ = 2 M). The solution was then transferred to a 10 mL test tube equipped with a magnetic stir bar and rubber septum, degassed via three freeze−pump−thaw cycles, and backfilled with argon. An initial aliquot (200 μL) was taken prior to heating the reaction vessel at the indicated temperature with subsequent aliquots taken at timed intervals and analyzed by ^{1}H NMR (DMSO-d_6) to determine monomer conversion by comparing the relative integral areas of the trimesic acid aromatic protons (8.64 ppm, 3H) to the vinyl proton of PhMA (5.86 ppm, 1H) or BnMA (5.79 ppm, 1H). SEC-MALLS (DMF 20 mM LiBr) analysis of aliquots was used to monitor molecular weight and molecular weight distribution progression throughout each polymerization.

Trithiocarbonate Degradation Analysis by UV−Vis. Reactions (final volume = 2500 μL) were performed using $[CPDT]_0 = 5 \times 10^{-3}$ M and $[M]_0$:$[CPDT]_0$:$[V501]_0$ = 10:1:0.2 in DMF. A typical procedure was as follows: BnMA (250 μL of an 87.6 mg/mL stock solution in DMF, 10 equiv), CPDT (250 μL of a 17.3 mg/mL stock soln. in DMF, 1 equiv), V501 (25 μL of a 28.0 mg/mL stock solution in DMF, 0.2 equiv), and DMF (1975 μL) were combined in a 4 mL test tube equipped with magnetic stir bar and rubber septum. The reaction was then degassed via four freeze−pump−thaw cycles and backfilled under argon. An initial aliquot (50 μL) was taken using an argon-purged gastight syringe and subsequently diluted into a quartz cuvette containing 2500 μL of acetonitrile before measuring the absorbance at λ = 320 nm using a Lambda 35 UV−vis spectrometer. Subsequent aliquots (50 μL) were taken and analyzed in the same manner.

***In Situ* ^{1}H NMR Analysis.** Samples of CPDT-PhMA and CPDT-BnMA (2×10^{-2} M) in DMF-d_7 were prepared immediately prior to analysis by first adding DMF-d_7 (0.60 mL) into an NMR tube equipped with pierceable rubber septum, and the solvent was degassed by two freeze−pump−thaw cycles to remove possible traces of dimethylamine. The appropriate amount of CPDT-PhMA or CPDT-BnMA was then added as a solid directly into the NMR tube containing the previously degassed DMF-d_7, and the resulting solution was degassed by two additional freeze−pump−thaw cycles and backfilled with argon. ^{1}H NMR spectra were acquired at 70 °C using a Bruker Ascend 600 MHz spectrometer.

RESULTS AND DISCUSSION

PhMA and BnMA Polymerization Kinetics. To our knowledge, there are no reports detailing the effects of *N*-aryl substitution on RAFT-mediated polymerization control of (meth)acrylamides. To this end, we chose to compare the RAFT polymerizations of *N*-phenylmethacrylamide (PhMA) and *N*-benzylmethacrylamide (BnMA) under analogous conditions (Scheme 1). BnMA was chosen based upon its structural similarity to PhMA while lacking direct *N*-aryl substitution.

Scheme 1. Synthetic Route for CPDT-Mediated Polymerization of PhMA and BnMA in DMF at 70 or 30 °C

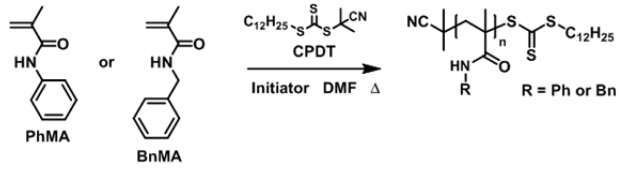

Table 1 summarizes the conversion, molar mass, and molecular weight distribution data for the polymerizations of PhMA and BnMA in DMF at 70 and 30 °C, using the RAFT agent 2-cyano-2-propyldodecyl trithiocarbonate (CPDT). The effect of methacrylamide structure on polymerization control is initially apparent by comparing the increase in molecular weight distribution of poly(PhMA) (M_w/M_n = 1.30) relative to that of poly(BnMA) (M_w/M_n = 1.15) synthesized under identical reaction conditions. Limited molecular weight control during polymerization of PhMA at 70 °C can also be seen in the M_n vs conversion plot (Supporting Information, Figure S1) which shows a decrease in $M_{n,exp}$ relative to $M_{n,th}$ at higher conversions. By contrast, for the polymerization of BnMA at 70 °C, $M_{n,exp}$ values mirror $M_{n,th}$ values, indicating that the number of active/dormant chain ends remain constant during polymerization (Figure S2).

Figure 1 shows the kinetic plots for the 70 °C polymerizations of PhMA (black) and BnMA (red); each plot shows an

DOI: 10.1021/acs.macromol.5b02463
Macromolecules 2016, 49, 465−474

Table 1. Conversion, Molar Mass, and Molecular Weight Distribution Data for the RAFT Polymerizations of PhMA and BnMA in DMF at 70 and 30 °C[a]

entry	monomer	temp (°C)	time (min)	conv[b] (%)	$M_{n,th}$[c] (g/mol)	$M_{n,exp}$[d] (g/mol)	M_w/M_n[d]
1a	PhMA	70	240	37	12400	14800	1.09
1b	PhMA	70	360	48	16000	17300	1.16
1c	PhMA	70	480	55	18200	18100	1.24
1d	PhMA	70	600	59	19500	18900	1.30
2a	BnMA	70	240	24	8900	11700	1.06
2b	BnMA	70	360	32	11500	13400	1.11
2c	BnMA	70	480	37	13400	15000	1.15
2d	BnMA	70	600	41	14600	16100	1.15
3a	PhMA	30	300	9	3200	6000	1.07
3b	PhMA	30	420	14	4900	7400	1.05
3c	PhMA	30	600	23	7800	10500	1.02
3d	PhMA	30	1380	50	16600	18800	1.02
4a	BnMA	30	300	7	2700	3400	1.13
4b	BnMA	30	420	10	3700	4100	1.07
4c	BnMA	30	600	14	5100	5900	1.05
4d	BnMA	30	1380	29	10400	11200	1.04

[a]Polymerizations were conducted at 70 or 30 °C in DMF ($[M]_0$:$[CTA]_0$:$[I]_0$ = 200:1.0:0.2) using V501 or V-70 as the initiators, respectively. [b]Conversions were determined by ^{1}H NMR (DMSO-d_6) by comparing the relative integral areas of trimesic acid (internal standard) aromatic protons (8.64 ppm, 3H) to the vinyl proton of PhMA (5.86 ppm, 1H) or BnMA (5.79 ppm, 1H). [c]Theoretical M_n values were calculated according to the equation $M_{n,th} = (\rho MW_{mon}[M]_0/[CTA]_0) + MW_{CTA}$ where ρ is the fractional monomer conversion, MW_{mon} is the molecular weight of the monomer, and MW_{CTA} is the molecular weight of the CTA. [d]Experimental M_n and M_w/M_n values were determined by SEC-MALLS (DMF, 20 mM LiBr).

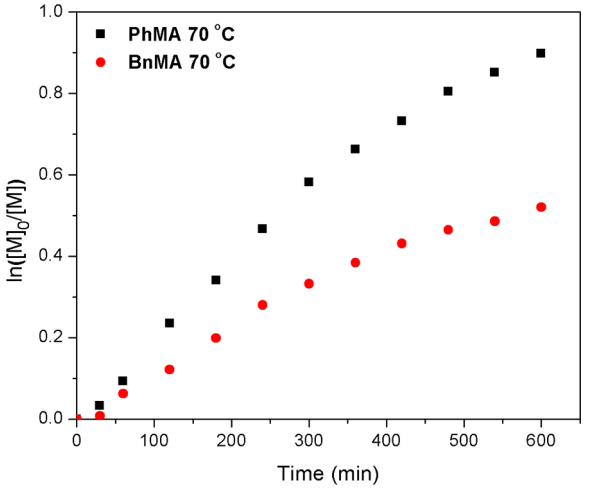

Figure 1. Kinetic plot for the CPDT-mediated polymerization of PhMA and BnMA in DMF at 70 °C ($[M]_0$ = 2.0 M, $[M]_0$:$[CTA]_0$:$[I]_0$ = 200:1:0.2).

initialization period of approximately 30 min followed by pseudo-first-order kinetic behavior up to 300 min with the differences in slope of the curves indicative of the relative propagation rate coefficients (k_p) for each monomer derivative. Similar initialization periods were observed previously for the trithiocarbonate-mediated polymerizations of *N*-aryl MSAs and are indicative of slow fragmentation/reinitiation by the RAFT agent R-group.[20,33] Interestingly, the first-order kinetic plots for the homopolymerizations of PhMA and BnMA at 70 °C show similar minimal decreases in slope beyond 300 min despite limited molecular weight control observed during the same time period for the polymerization of PhMA. It might be expected that RAFT agent degradation during polymerization of PhMA would result in a decrease in the slope ($k_p[P_n^\bullet]$) of the pseudo-first-order kinetic plot due to chain transfer to thiol-containing degradation byproducts. However, efficient chain transfer can take place without influencing the rate of polymerization if the rate of reinitiation by thiyl radicals is greater than the rate of propagation (i.e., $k_{iT} > k_p$).[34] The decrease in $M_{n,exp}$ relative to $M_{n,th}$ throughout the 70 °C polymerization of PhMA (Figure S1) is evidence of an increasing number of polymer chains resulting from efficient chain transfer.

Recently we demonstrated that improved chain end retention and narrow molecular weight distributions can be achieved during the RAFT polymerization of *N*-aryl MSAs by reducing the reaction temperature.[20] Likewise, as seen in Figure 2, the molecular weight distribution of poly(PhMA) synthesized at 30 °C (M_w/M_n = 1.02, M_n = 18 800) was markedly narrower than that of poly(PhMA) synthesized under analogous conditions at 70 °C (M_w/M_n = 1.30, M_n = 18 900). Reduced polymerization temperature also afforded improved molecular weight control during the polymerization of PhMA as evidenced by the linear progression of $M_{n,exp}$ with conversion and good correlation between $M_{n,exp}$ and $M_{n,th}$ values (Figure S3). As shown in Table 1, narrower molecular weight distributions were also obtained during the polymerization of BnMA at 30 °C (M_w/M_n < 1.10), but the additional decrease was minimal due to already narrow M_w/M_n achieved during polymerization at 70 °C.

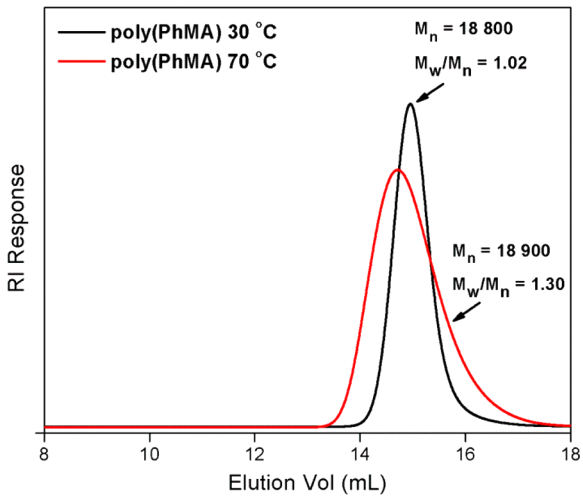

Figure 2. SEC RI chromatogram showing the effect of temperature on molecular weight distribution for the CPDT-mediated RAFT polymerization of PhMA in DMF at 70 and 30 °C.

The kinetic plots for the CPDT-mediated polymerizations of PhMA and BnMA at 30 °C (Figure 3) exhibit initialization times of 100 and 60 min, respectively, while demonstrating near pseudo-first-order kinetic behavior up to at least 1380 min. The increase in initialization time with decreasing temperature for the RAFT polymerizations of PhMA and BnMA is consistent with observations made by McLeary et al.[33] The improved linearity of the first-order kinetic plots is also consistent with

DOI: 10.1021/acs.macromol.5b02463
Macromolecules 2016, 49, 465−474

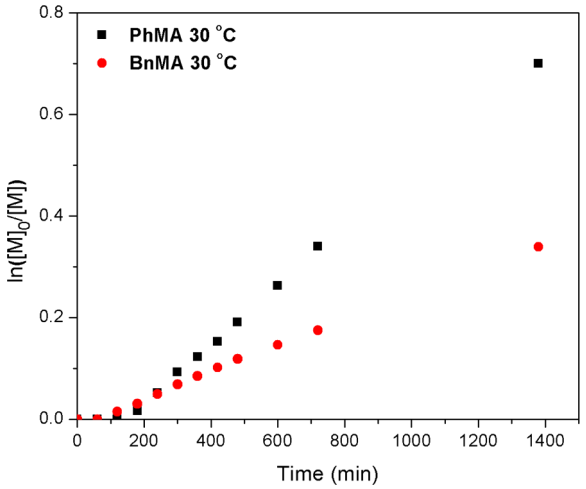

Figure 3. Kinetic plot for the CPDT-mediated polymerization of PhMA and BnMA in DMF at 30 °C ($[M]_0$ = 2.0 M, $[M]_0$:$[CTA]_0$:$[I]_0$ = 200:1:0.2).

previous low temperature RAFT polymerizations of (meth)-acrylamides and is generally attributed to increased thiocarbonylthio chain end retention.[35,36]

Trithiocarbonate Degradation during the CPDT-Mediated Polymerizations of PhMA and BnMA. It is evident from the molecular weight data summarized in Table 1 that chain end degradation is likely occurring during the 70 °C polymerization of PhMA. Meanwhile, BnMA polymerization at the same temperature affords narrower molecular weight distributions with good correlation between $M_{n,th}$ and $M_{n,exp}$ values. In order to ascertain the influences of each polymerization component (i.e., solvent, monomer, and initiator) on temperature-dependent trithiocarbonate degradation, reactions were performed in DMF using combinations of CPDT, monomer (PhMA or BnMA), and initiator (V501) at relative concentrations of $[CPDT]_0$:$[M]_0$:$[I]_0$ = 10:1.0:0.2 as illustrated in Figure 4. The fractional change in total trithiocarbonate (TTC) concentration ($[TTC]/[TTC]_0$) was measured by comparing the absorbance (λ = 320 nm) of diluted aliquots taken at timed intervals to that of an initial aliquot at t = 0. It is worth noting that only minimal change in the molar extinction coefficient (ε) of CPDT at λ = 320 nm occurs after covalent addition of PhMA or BnMA, allowing for accurate measurement of the total [TTC] during polymerization. Figure S5 shows the Beer–Lambert plots and ε values at λ = 320 nm for CPDT (ε_{320} = 9380 M^{-1} cm^{-1}) and the corresponding single monomer unit insertion adducts CPDT-PhMA (ε_{320} = 9560 M^{-1} cm^{-1}) and CPDT-BnMA (ε_{320} = 10 300 M^{-1} cm^{-1}).

Examination of Figure 4a reveals no measurable influences of DMF (green ▼), PhMA (blue ▲), or V501 (red ●) independently on $[TTC]/[TTC]_0$ at 70 °C. However, a 60% decrease in $[TTC]/[TTC]_0$ is observed after 12 h when CPDT, PhMA, and V501 are combined at 70 °C (black ■) such that monomer addition to CPDT takes place. This result supports terminal monomer unit-induced degradation in which the ultimate methacrylamide unit is in a favored orientation for O-5 or N-5 nucleophilic attack on the terminal thiocarbonyl (Scheme 2). In this case "5" denotes the number of atoms between the amide oxygen or nitrogen and the thiocarbonyl carbon. By contrast, identical experiments performed with BnMA showed minimal trithiocarbonate degradation during

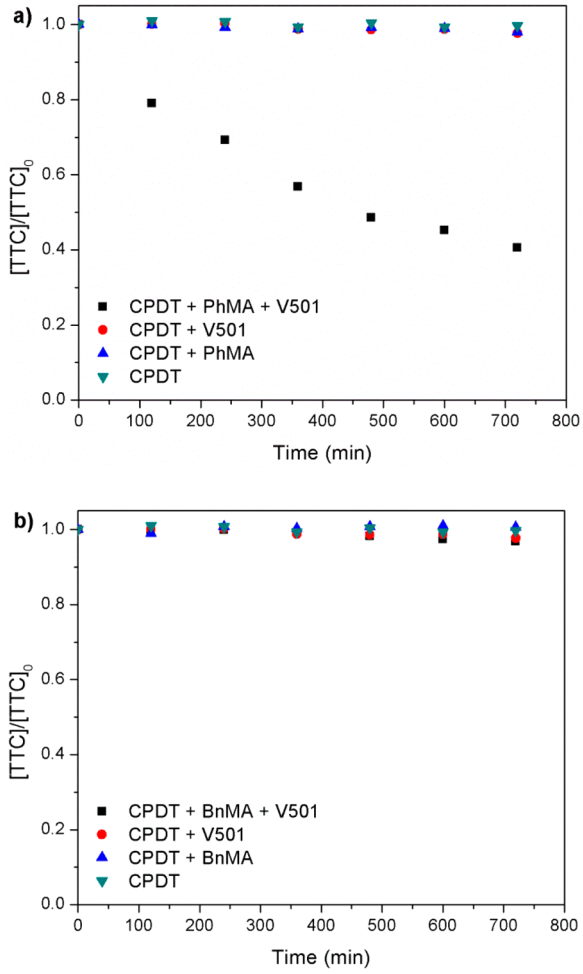

Figure 4. Individual and combined influences of solvent, initiator, and monomer on the time-dependent change in $[TTC]/[TTC]_0$ as measured by UV–vis spectroscopy ($[M]_0$:$[CTA]_0$:$[I]_0$ = 10:1:0.2). Trithiocarbonate degradation experiments were performed using (a) PhMA or (b) BnMA as the monomer.

Scheme 2. Proposed Trithiocarbonate Degradation by O-5 or N-5 Nucleophilic Attack by the Terminal Methacrylamide Unit

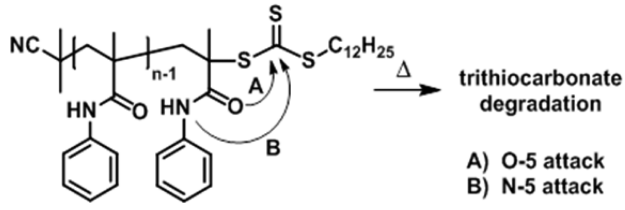

polymerization with only a 3% decrease in $[TTC]/[TTC]_0$ observed after 12 h.

Previously, we attributed the substantially improved polymerization control of MSAs and PhMA at 30 °C to increased chain end retention.[20] As seen in Figure 5, the effect of temperature on trithiocarbonate degradation was confirmed by measuring $[TTC]/[TTC]_0$ during polymerization of PhMA at 30 °C under analogous conditions used for experiments in Figure 4a. At 30 °C, only 8% trithiocarbonate degradation was observed after 720 min compared to 60% degradation for the same time period at 70 °C.

DOI: 10.1021/acs.macromol.5b02463
Macromolecules 2016, 49, 465–474

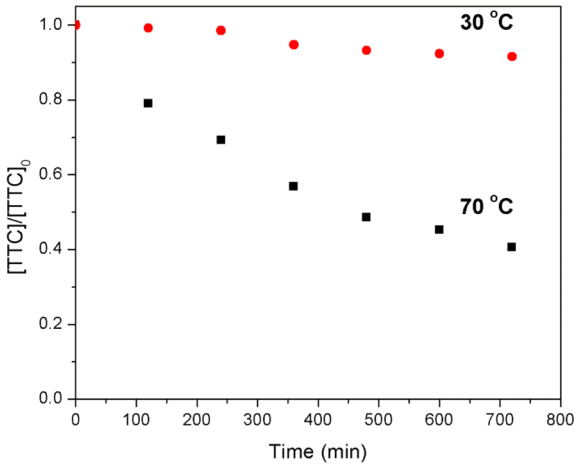

Figure 5. Trithiocarbonate degradation during the CPDT-mediated polymerization of PhMA ($[M]_0$:$[CTA]_0$:$[I]_0$ = 10:1:0.2) at 70 and 30 °C using V501 and V-70 as initiators, respectively.

Small Molecule Analogue Synthesis. In order to better study the mechanism and byproducts of *N*-arylmethacrylamide-promoted trithiocarbonate degradation, we attempted to synthesize a small molecule analogue of trithiocarbonate-terminated poly(PhMA). According to Scheme 3, the desired

Scheme 3. Synthetic Route for the Trithiocarbonate-Terminated Poly(PhMA) Small Molecule Analogue 8

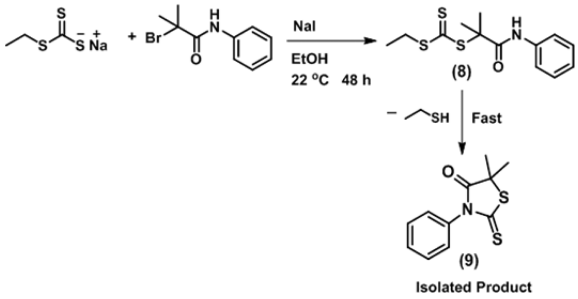

product **8** should result from the SN_1 reaction of sodium ethyl trithiocarbonate and 2-bromoisobutyranilide. Despite the reaction being performed at room temperature (22 °C), isolation of **8** proved unsuccessful. Recrystallization of the crude reaction mixture afforded 5,5-dimethyl-3-phenyl-2-thioxothiazolidin-4-one (**9**), the N-5 cyclization product of **8** (Scheme 3). The structure of **9** was confirmed in part by analysis of the ^{1}H NMR spectrum (Figure 6) which is absent of ethylsulfanyl $-SCH_2CH_3$ and amide $-N-H$ ^{1}H resonances. The ^{1}H and ^{13}C chemical shifts of **9** match those reported previously.[32] ^{1}H NMR analysis of aliquots sampled during the reaction (Scheme 3) showed rapid formation of **9**, indicating that under these conditions N-5 cyclization/elimination of the transient species **8** occurs even at temperatures below 30 °C.

Small Molecule Analogue Synthesis via Single Monomer Unit Insertion. Minimal degradation of CPDT during the polymerization of PhMA at 30 °C indicates that covalent adducts of PhMA and CPDT are stable at low temperatures and can be formed by free radical processes. Recently, single monomer unit insertion (SMUI)[37,38] has become a facile method for CTA synthesis, exploiting the "initialization" phenomenon previously described by McLeary, Klumperman, and co-workers.[33] We found that the SMUI

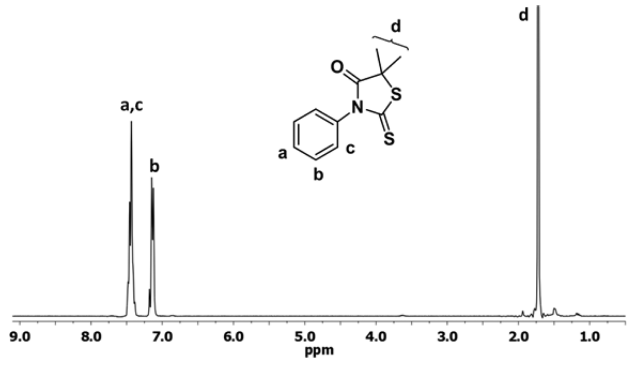

Figure 6. ^{1}H NMR (300 MHz, $CDCl_3$) spectrum of isolated N-5 cyclization/elimination product **9**.

adduct of CPDT and PhMA (CPDT-PhMA) could be marginally favored by stoichiometric control of monomer, CTA, and initiator at 30 °C as outlined in Scheme 4. The

Scheme 4. Synthesis of CPDT-PhMA and CPDT-BnMA by Single Monomer Unit Insertion

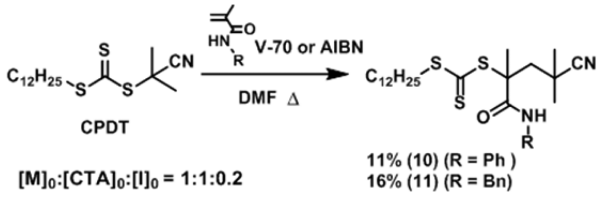

SMUI adduct of CPDT and BnMA (CPDT-BnMA) was synthesized at 60 °C using AIBN as the initiator owing to the lower nucleophilicity of the *N*-benzylamide at higher temperatures as previously demonstrated. The labeled ^{1}H NMR spectra of CPDT-PhMA (**10**) and CPDT-BnMA (**11**) are shown in Figures 7a and 7b, respectively.

***In Situ* ^{1}H NMR Analysis of CPDT-PhMA and CPDT-BnMA Degradation at 70 °C.** *In situ* ^{1}H NMR analysis was used to gain further insight into the mechanism and kinetics of CPDT-PhMA and CPDT-BnMA degradation. The labeled ^{1}H NMR spectra at select time points during the degradation analysis of CPDT-PhMA at 70 °C in DMF-d_7 are shown in Figure 8. After 5 min, only the ^{1}H resonances of CPDT-PhMA are observed. Subsequently, new signals in the aromatic (7.4–7.7 ppm) and aliphatic (1.5–2.7 ppm) regions corresponding to degradation byproducts appear and increase in intensity with time. Comparison of the ^{1}H NMR chemical shifts of the degradation byproducts (Figure 8) with those of 1-dodecanethiol and 5,5-dimethyl-3-phenyl-2-thioxothiazolidin-4-one (**9**) (Figures S6–S8) indicates that the byproducts of CPDT-PhMA degradation are those formed exclusively by N-5 cyclization/elimination. Labeled resonances corresponding to N-5 cyclization/elimination degradation byproducts are given prime designation in the NMR spectrum (Figure 8) obtained at 491 min.

Degradation of CPDT-BnMA at 70 °C (Figure 9) was also monitored using *in situ* ^{1}H NMR analysis. After 491 min, minimal degradation was observed as shown in the expanded regions of the ^{1}H NMR spectrum in Figure 9 corresponding to the 3-benzyl-2-thioxothiazolidin-4-one methylene (peak i′) and the cyclized BnMA methyl (peak e′). Also visible is the characteristic methylene of 1-dodecanethiol (peak d′) which is

DOI: 10.1021/acs.macromol.5b02463
Macromolecules 2016, 49, 465–474

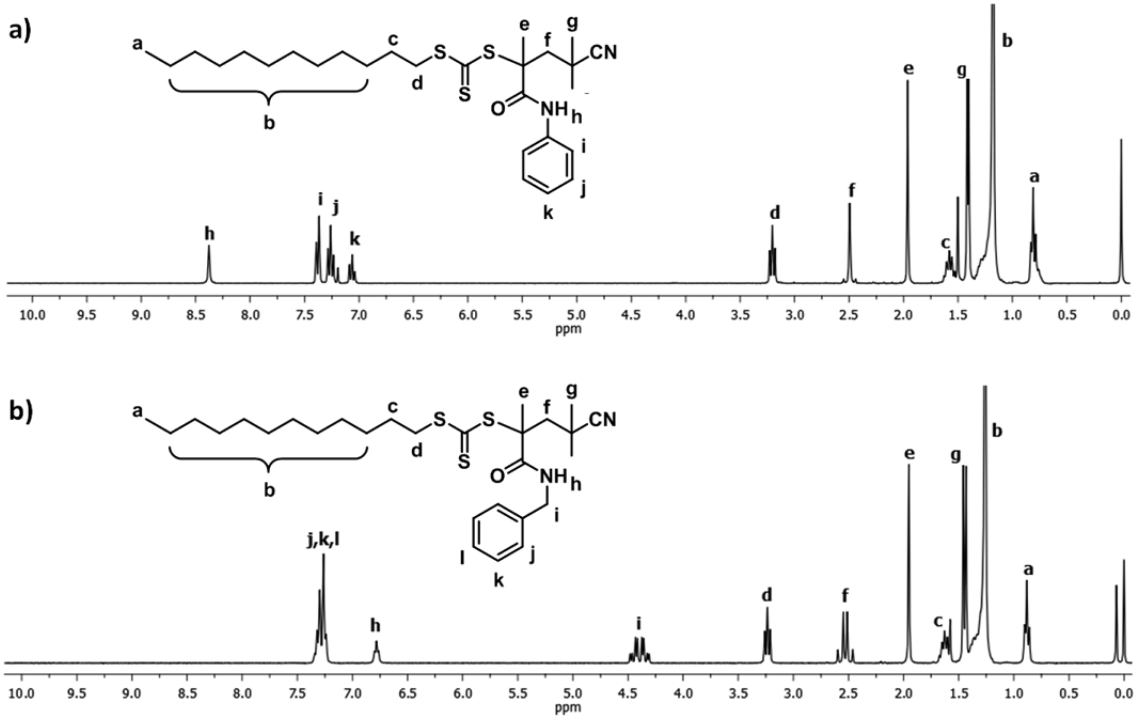

Figure 7. ^{1}H NMR (300 MHz, $CDCl_3$) spectra of (a) CPDT-PhMA and (b) CPDT-BnMA SMUI adducts.

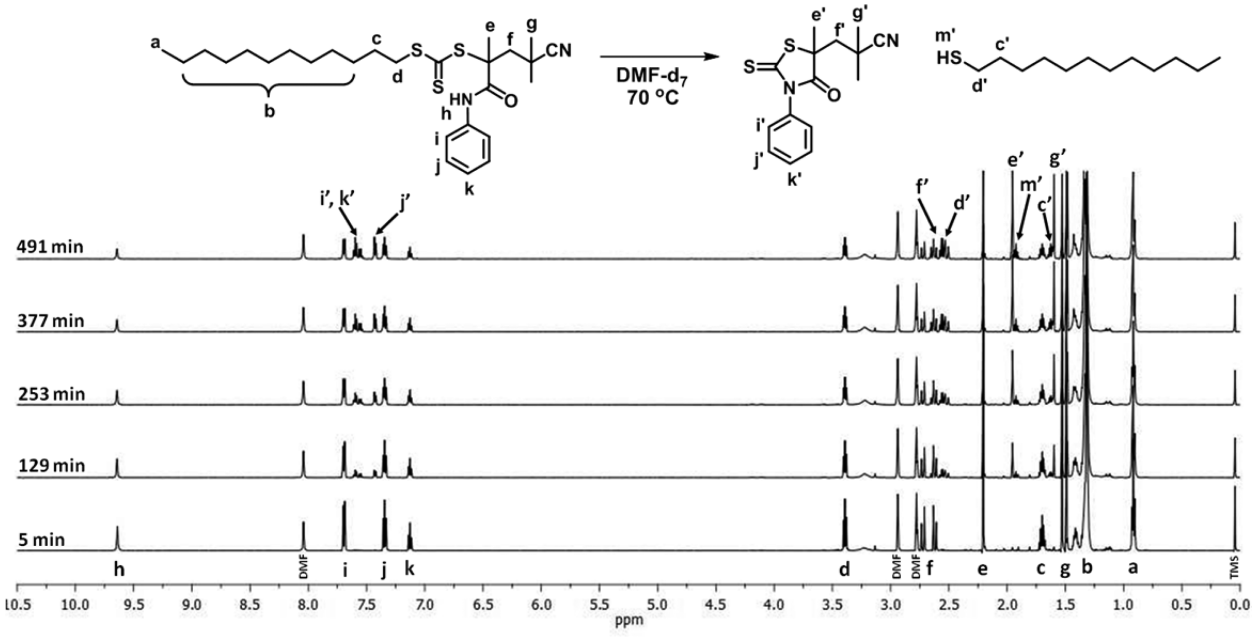

Figure 8. ^{1}H NMR (600 MHz, DMF-d_7) overlay following the time-dependent degradation of CPDT-PhMA at 70 °C.

additional evidence of degradation by N-5 cyclization/elimination.

Kinetic analysis of CPDT-PhMA degradation also provides additional evidence for exclusive N-5 cyclization/elimination. As shown in Scheme 5, intramolecular N-5 nucleophilic attack of the trithiocarbonate by adjacent methacrylamide can occur by either cyclization/elimination (pathway A) or rearrangement (pathway B) depending upon which C−S bond is cleaved. The total rate of degradation of CPDT-PhMA by pathways A and B is equal to the rate of change in area of the phenyl ^{1}H resonances (Figure 8, peaks i, j, and k) as N-5 nucleophilic attack results in loss of the *N*-phenylamide. The exclusive rate of N-5 cyclization/elimination (pathway A) is equal to the rate of change in area of the $-CH_2-S-$ ^{1}H resonance (Figure 8, peak d) as elimination of 1-dodecanethiol occurs. As shown in Figure 10a, the fractional changes in area (A_t/A_0) of peaks i (7.70 ppm) and d (3.39 ppm) are essentially identical throughout the 491 min experiment, indicating that pathway A is the predominant contributor to the degradation of CPDT-PhMA at 70 °C.

Kinetic analysis of CPDT-BnMA degradation (Figure 10b) additionally supports the proposed degradation pathway of N-5

DOI: 10.1021/acs.macromol.5b02463
Macromolecules 2016, 49, 465−474

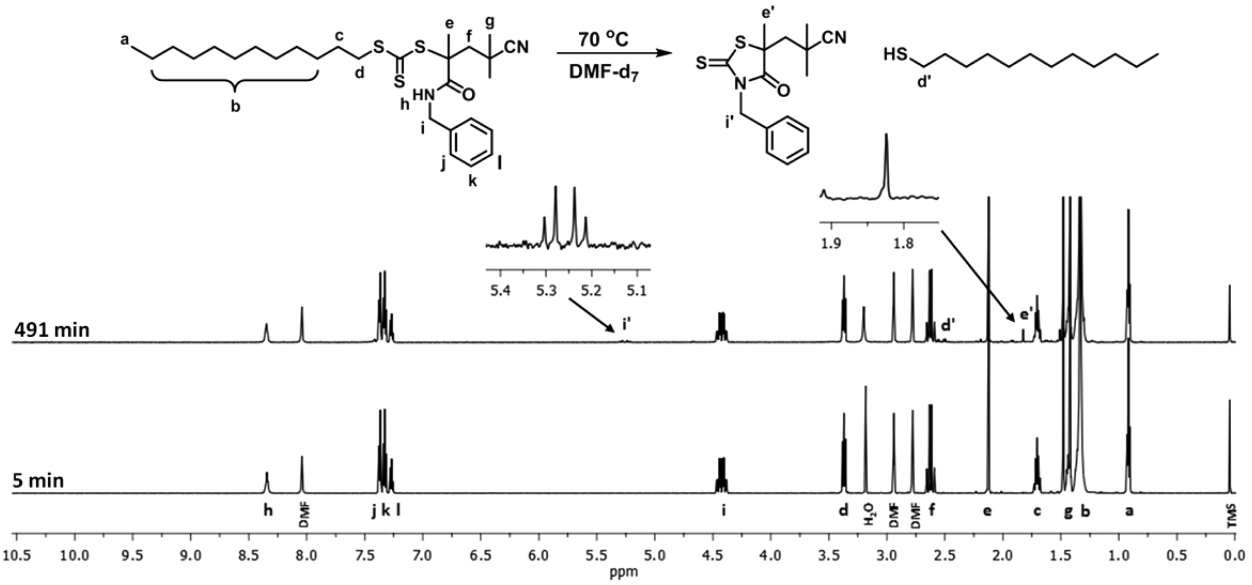

Figure 9. ^{1}H NMR (600 MHz, DMF-d_7) overlay following the time-dependent degradation of CPDT-BnMA at 70 °C.

Scheme 5. Possible N-5 Nucleophilic Attack Degradation Pathways

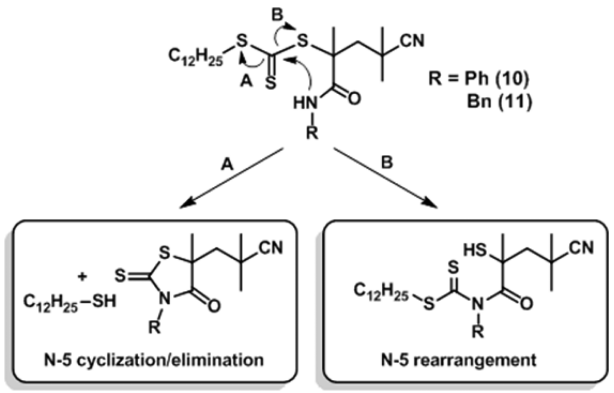

cyclization/elimination as shown by the comparable change in A_t/A_0 of peaks i (4.42 ppm) and d (3.37 ppm) (peak assignments in Figure 9).

As seen in Figure 11, excellent agreement is observed between the time-dependent fractional changes in [TTC] measured during the CPDT-mediated polymerizations of PhMA and BnMA by UV−vis spectroscopy (open data points) and during CPDT-PhMA and CPDT-BnMA degradation measured by *in situ* ^{1}H NMR analysis (solid data points). The half-lives ($t_{1/2}$) of CPDT-PhMA and CPDT-BnMA at 70 °C in DMF were calculated to be $t_{1/2}$ = 7.18 h and $t_{1/2}$ = 78.5 h, respectively, based upon the degradation rates measured using ^{1}H NMR.

It is important to note that while we have determined that significant trithiocarbonate degradation occurs by N-5 cyclization/elimination during the RAFT polymerization of PhMA at 70 °C, this work does not specifically address the influence of *N*-phenyl substitution on increased amide nucleophilicity and how this affects the observed reaction mechanism. We are currently examining the influences of *N*-aryl substitution on both reaction mechanism and rate of N-5 cyclization/elimination and will report this in a future paper.

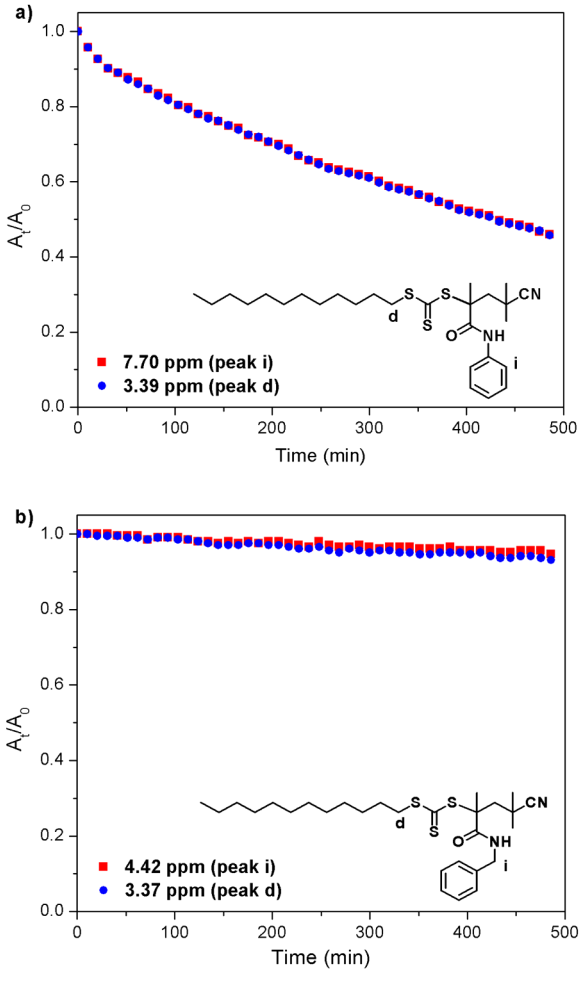

Figure 10. Time-dependent fractional change in the area of select ^{1}H chemical shifts during the degradation of (a) CPDT-PhMA and (b) CPDT-BnMA in DMF-d_7 at 70 °C.

Influence of 3-Phenyl-2-thioxothiazolidin-4-one Chain Ends on RAFT Polymerization of PhMA. Typically, RAFT agent degradation during polymerization results in the

DOI: 10.1021/acs.macromol.5b02463
Macromolecules 2016, 49, 465−474

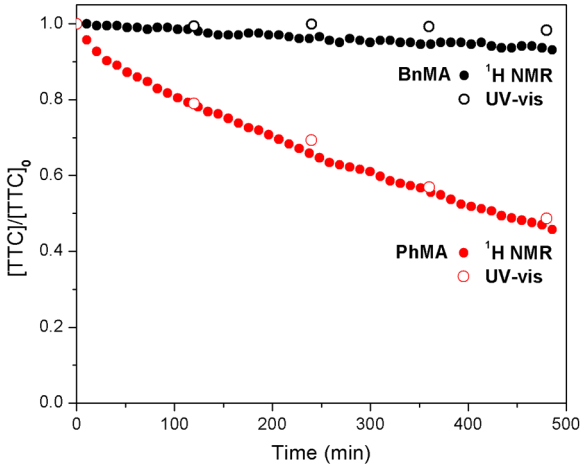

Figure 11. Time-dependent change in $[TTC]/[TTC]_0$ at 70 °C in DMF as measured by UV−vis spectroscopy during polymerization (open circles) and as measured by *in situ* ^{1}H NMR during SMUI adduct degradation analysis (closed circles).

loss of active thiocarbonylthio chain ends affording "dead" polymer chains that can no longer participate in the RAFT process. However, we have shown that trithiocarbonate degradation by N-5 cyclization/elimination during the polymerization PhMA results in formation of a new cyclic thiocarbonylthio end group. To date, there are few examples of RAFT polymerizations mediated by cyclic thiocarbonylthio compounds.[39−41] However, Zhan and co-workers recently reported the RAFT polymerization of vinyl acetate using **9** as the RAFT agent, which resulted in incorporation of thiocarbonylthio functionality into the polymer backbone.[32] Similarly, it is plausible that the 3-phenyl-2-thioxothiazolidin-4-one chain ends formed as a result of N-5 cyclization/elimination could participate during the RAFT polymerization of PhMA as shown in Scheme 6.

We investigated the possibility of 3-phenyl-2-thioxothiazolidin-4-one chain ends participating in the RAFT process by conducting the polymerization of PhMA at 70 °C in the presence of **9**, a small molecule analogue of N-5 cyclized poly(PhMA) chain ends. Figure 12a shows the kinetic plot for the **9**-mediated polymerization of PhMA in DMF at 70 °C.

Scheme 6. Proposed Mechanism for Radical Addition to 3-Phenyl-2-thioxothiazolidin-4-one Chain Ends during RAFT Polymerization of PhMA at 70 °C

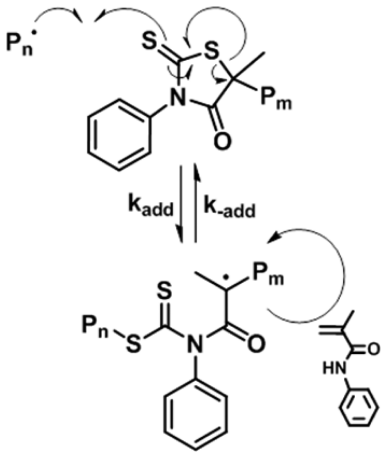

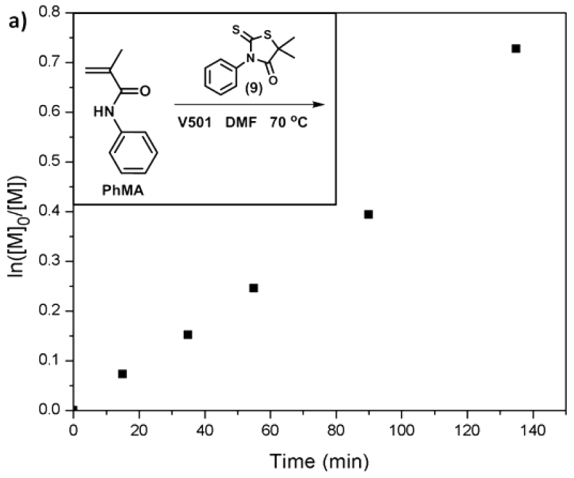

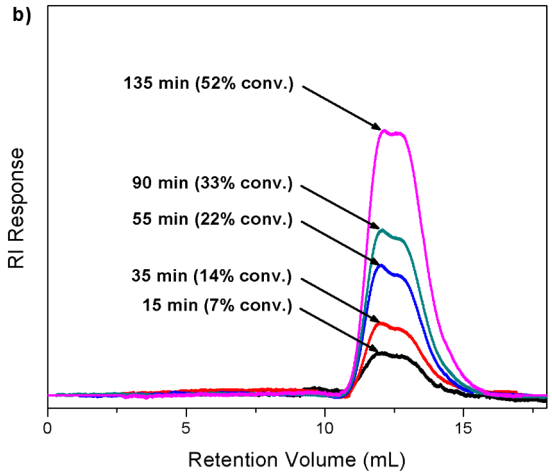

Figure 12. (a) Kinetic plot and (b) SEC RI chromatogram overlay for the **9**-mediated polymerization of PhMA in DMF at 70 °C ($[PhMA]_0$ = 2.0 M, $[PhMA]_0$:$[9]_0$:$[V501]_0$ = 200:1.0:0.2).

Linear pseudo-first-order kinetic behavior was observed up to 140 min with no initialization period. By contrast, the CPDT-mediated polymerization of PhMA under identical conditions exhibited a 30 min initialization period, consistent with similar results first reported by Klumperman and co-workers.[33] While the linear pseudo-first-order kinetic behavior indicates a constant $k_p[P_n^•]$, the SEC RI overlay shown in Figure 12b demonstrates that molecular weight control is not achieved during the **9**-mediated polymerization of PhMA at 70 °C. The intensities of the SEC RI chromatograms shown in Figure 12b increase with conversion, but the unchanging peak elution volumes, which occur at the exclusion limit of the SEC system (~11.0 mL), are representative of uncontrolled polymerization behavior where M_n does not scale linearly with monomer conversion. While the polymers presented in Figure 12b were too large to characterize by our SEC-MALLS system, it is worth noting that a polyvinylpyridine standard of M_n = 475 000 g/mol (M_w/M_n = 1.06) elutes at a volume of 11.5 mL. These results suggest that 3-phenyl-2-thioxothiazolidin-4-one-terminated polymers do not participate in the normal CTA-mediated RAFT polymerization of PhMA at 70 °C.

■ CONCLUSIONS

Methacrylamide-induced trithiocarbonate degradation during RAFT polymerization has been investigated. *N*-Phenyl-

DOI: 10.1021/acs.macromol.5b02463
Macromolecules 2016, 49, 465−474

promoted nucleophilic attack of the terminal trithiocarbonate by the ultimate methacrylamide unit was shown to occur by N-5 cyclization/elimination, resulting in rapid loss of active chain ends in DMF at 70 °C. The 3-phenyl-2-thioxothiazolidin-4-one RAFT polymer chain ends resulting from N-5 cyclization/elimination were shown to have little direct influence on the RAFT process and thus function as "dead" chain ends. Suppression of methacrylamide-induced trithiocarbonate degradation during the RAFT polymerization of *N*-arylmethacrylamides can be achieved by reducing the reaction temperature to 30 °C. Work is currently underway in our laboratories to study the influence of *N*-aryl amide substitution on both the reaction mechanism and rate of N-5 cyclization/elimination.

■ ASSOCIATED CONTENT

Supporting Information

The Supporting Information is available free of charge on the ACS Publications website at DOI: 10.1021/acs.macromol.5b02463.

M_n versus conversion plots and additional ^{1}H NMR and UV−vis characterization of SMUI adducts and degradation byproducts (PDF)

■ AUTHOR INFORMATION

Corresponding Author

*E-mail: charles.mccormick@usm.edu (C.L.M.).

Notes

The authors declare no competing financial interest.

■ ACKNOWLEDGMENTS

The authors gratefully acknowledge the financial support provided in part by the National Science Foundation Graduate Research Fellowship Program under Grant GM004636/GR04355 and the National Science Foundation's ESPSCoR under Agreement IIA1430364.

■ REFERENCES

(1) Hawker, C. J.; Bosman, A. W.; Harth, E. *Chem. Rev.* **2001**, *101*, 3661−3688.
(2) Matyjaszewski, K. *Macromolecules* **2012**, *45*, 4015−4039.
(3) Moad, G.; Rizzardo, E.; Thang, S. H. *Polymer* **2008**, *49*, 1079−1131.
(4) Lowe, A. B.; McCormick, C. L. *Prog. Polym. Sci.* **2007**, *32*, 283−351.
(5) Qiu, X. P.; Winnik, F. M. *Macromol. Rapid Commun.* **2006**, *27*, 1648−1653.
(6) Pretula, J.; Kaluzynski, K.; Wisniewski, B.; Szymanski, R.; Loontjens, T.; Penczek, S. *J. Polym. Sci., Part A: Polym. Chem.* **2008**, *46*, 830−843.
(7) Inglis, A. J.; Sinnwell, S.; Davis, T. P.; Barner-Kowollik, C.; Stenzel, M. H. *Macromolecules* **2008**, *41*, 4120−4126.
(8) Li, M.; De, P.; Gondi, S. R.; Sumerlin, B. S. *J. Polym. Sci., Part A: Polym. Chem.* **2008**, *46*, 5093−5100.
(9) Boyer, C.; Bulmus, V.; Davis, T. P. *Macromol. Rapid Commun.* **2009**, *30*, 493−497.
(10) Boyer, C.; Granville, A.; Davis, T. P.; Bulmus, V. *J. Polym. Sci., Part A: Polym. Chem.* **2009**, *47*, 3773−3794.
(11) Tasdelen, M. A.; Kahveci, M. U.; Yagci, Y. *Prog. Polym. Sci.* **2011**, *36*, 455.
(12) Thomas, D. B.; Convertine, A. J.; Hester, R. D.; Lowe, A. B.; McCormick, C. L. *Macromolecules* **2004**, *37*, 1735−1741.
(13) Thomas, D. B.; Convertine, A. J.; Myrick, L. J.; Scales, C. W.; Smith, A. E.; Lowe, A. B.; Vasilieva, Y. A.; Ayres, N.; McCormick, C. L. *Macromolecules* **2004**, *37*, 8941−8950.
(14) Zhou, Y.; He, J.; Li, C.; Hong, L.; Yang, Y. *Macromolecules* **2011**, *44*, 8446−8457.
(15) Gruendling, T.; Pickford, R.; Guilhaus, M.; Barner-Kowollik, C. *J. Polym. Sci., Part A: Polym. Chem.* **2008**, *46*, 7447−7461.
(16) Li, C.; He, J.; Zhou, Y.; Gu, Y.; Yang, Y. *J. Polym. Sci., Part A: Polym. Chem.* **2011**, *49*, 1351−1360.
(17) Monteiro, M. J.; de Brouwer, H. *Macromolecules* **2001**, *34*, 349−352.
(18) Bathfield, M.; D'Agosto, F.; Spitz, R.; Ladavière, C.; Charreyre, M. T.; Delair, T. *Macromol. Rapid Commun.* **2007**, *28*, 856−862.
(19) Favier, A.; Ladavière, C.; Charreyre, M. T.; Pichot, C. *Macromolecules* **2004**, *37*, 2026−2034.
(20) Abel, B. A.; Sims, M. B.; McCormick, C. L. *Macromolecules* **2015**, *48*, 5487−5495.
(21) Chong, B. Y. K.; Le, T. P. T.; Moad, G.; Rizzardo, E.; Thang, S. H. *Macromolecules* **1999**, *32*, 2071−2074.
(22) Pai, T. S. C.; Barner-Kowollik, C.; Davis, T. P.; Stenzel, M. H. *Polymer* **2004**, *45*, 4383−4389.
(23) Schilli, C.; Lanzendörfer, M. G.; Müller, A. H. E. *Macromolecules* **2002**, *35*, 6819−6827.
(24) Donovan, M. S.; Lowe, A. B.; Sumerlin, B. S.; McCormick, C. L. *Macromolecules* **2002**, *35*, 4123−4132.
(25) Donovan, M. S.; Sanford, T. A.; Lowe, A. B.; Sumerlin, B. S.; Mitsukami, Y.; McCormick, C. L. *Macromolecules* **2002**, *35*, 4570−4572.
(26) Teodorescu, M.; Matyjaszewski, K. *Macromolecules* **1999**, *32*, 4826−4831.
(27) Rademacher, J. T.; Baum, M.; Pallack, M. E.; Brittain, W. J.; Simonsick, W. J. *Macromolecules* **2000**, *33*, 284−288.
(28) Alsubaie, F.; Anastasaki, A.; Wilson, P.; Haddleton, D. M. *Polym. Chem.* **2015**, *6*, 406−417.
(29) Montalbetti, C. A. G. N.; Falque, V. *Tetrahedron* **2005**, *61*, 10827−10852.
(30) Edman, P. *Acta Chem. Scand.* **1950**, *4*, 283−293.
(31) Cunningham, B. A.; Schmir, G. L. *J. Org. Chem.* **1966**, *31*, 3751−3754.
(32) Zhan, Y.; Zhang, Z.; Pan, X.; Zhu, J.; Zhou, N.; Zhu, X. *J. Polym. Sci., Part A: Polym. Chem.* **2013**, *51*, 1656−1663.
(33) McLeary, J. B.; Calitz, F. M.; McKenzie, J. M.; Tonge, M. P.; Sanderson, R. D.; Klumperman, B. *Macromolecules* **2004**, *37*, 2383−2394.
(34) Moad, G.; Solomon, D. H. *The Chemistry of Radical Polymerization*, 2nd ed.; Elsevier Ltd.: Amsterdam, 2006.
(35) Convertine, A. J.; Ayres, N.; Scales, C. W.; Lowe, A. B.; McCormick, C. L. *Biomacromolecules* **2004**, *5*, 1177−1180.
(36) Convertine, A. J.; Lokitz, B. S.; Lowe, A. B.; Scales, C. W.; Myrick, L. J.; McCormick, C. L. *Macromol. Rapid Commun.* **2005**, *26*, 791−795.
(37) Houshyar, S.; Keddie, D. J.; Moad, G.; Mulder, R. J.; Saubern, S.; Tsanaktsidis, J. *Polym. Chem.* **2012**, *3*, 1879−1889.
(38) Vandenbergh, J.; Reekmans, G.; Adriaensens, P.; Junkers, T. *Chem. Commun.* **2013**, *49*, 10358−10360.
(39) Hong, J.; Wang, Q.; Lin, Y.; Fan, Z. *Macromolecules* **2005**, *38*, 2691−2695.
(40) Zhang, L.; Want, Q.; Lei, P.; Wang, X.; Wang, C.; Cai, L. *J. Polym. Sci., Part A: Polym. Chem.* **2007**, *45*, 2617−2623.
(41) Hong, J.; Wang, Q.; Fan, Z. *Macromol. Rapid Commun.* **2006**, *27*, 57−62.

DOI: 10.1021/acs.macromol.5b02463
Macromolecules 2016, 49, 465−474